

Regional Variation of CH₄ and N₂ Production Processes in the Deep Aquifers of an Accretionary Prism

MAKOTO MATSUSHITA¹, SHUGO ISHIKAWA², KAZUSHIGE NAGAI², YUICHIRO HIRATA², KUNIO OZAWA³, SATOSHI MITSUNOBU⁴, and HIROYUKI KIMURA^{1,2,3,5*}

¹Department of Environment and Energy Systems, Graduate School of Science and Technology, Shizuoka University, Oya, Suruga-ku, Shizuoka 422–8529, Japan; ²Department of Geosciences, Faculty of Science, Shizuoka University, Oya, Suruga-ku, Shizuoka 422–8529, Japan; ³Center for Integrated Research and Education of Natural Hazards, Shizuoka University, Oya, Suruga-ku, Shizuoka 422–8529, Japan; ⁴Department of Environmental Conservation, Graduate School of Agriculture, Ehime University, Tarumi, Matsuyama 790–8566, Japan; and ⁵Research Institute of Green Science and Technology, Shizuoka University, Oya, Suruga-ku, Shizuoka 422–8529, Japan

(Received May 14, 2016—Accepted July 8, 2016—Published online September 3, 2016)

Accretionary prisms are mainly composed of ancient marine sediment scraped from the subducting oceanic plate at a convergent plate boundary. Large amounts of anaerobic groundwater and natural gas, mainly methane (CH₄) and nitrogen gas (N₂), are present in the deep aquifers associated with an accretionary prism; however, the origins of these gases are poorly understood. We herein revealed regional variations in CH₄ and N₂ production processes in deep aquifers in the accretionary prism in Southwest Japan, known as the Shimanto Belt. Stable carbon isotopic and microbiological analyses suggested that CH₄ is produced through the non-biological thermal decomposition of organic matter in the deep aquifers in the coastal area near the convergent plate boundary, whereas a syntrophic consortium of hydrogen (H₂)-producing fermentative bacteria and H₂-utilizing methanogens contributes to the significant production of CH₄ observed in deep aquifers in midland and mountainous areas associated with the accretionary prism. Our results also demonstrated that N₂ production through the anaerobic oxidation of organic matter by denitrifying bacteria is particularly prevalent in deep aquifers in mountainous areas in which groundwater is affected by rainfall.

Key words: accretionary prism, deep aquifer, methanogens, fermentative bacteria, denitrification

Sequences in the accretionary prism of the non-subducting continental crust are thick sediments that were originally deposited on the subducting ocean plate. During subduction, parts of the marine sediment on the ocean plate are scraped off and accreted into an accretionary prism in the overlying continental plate (56). Accretionary prisms have been reported at convergent plate boundaries around the world, including those at Alaska and Washington in the U.S., New Zealand, Chile, Peru, Indonesia, Taiwan, and Japan (13, 21, 27).

The accretionary prism in southwest Japan, known as the Shimanto Belt, is composed of marine sediments deposited on the Philippine Sea Plate during the Cretaceous and Tertiary Periods (27, 55). The sediment structure is currently distributed in a wide region from the coastal area of the Pacific Ocean side to the mountainous area, and is traceable for 1,800 km in southwest Japan (Fig. 1). This accretionary prism is derived from ancient marine sediment scraped from the subducting ocean plate, and, thus, is rich in complex organic compounds (28). This sediment contains layers of water-bearing permeable sandstone and water-impermeable shale. Groundwater in this region is recharged by rainfall and seawater, which infiltrates outcrops or faults and is anaerobically reserved in deep aquifers (29). In addition to anaerobic groundwater, a large amount of natural gas, mainly methane (CH₄), has been detected in deep aquifers (29, 47).

CH₄ is an important greenhouse gas and energy resource

generated predominantly by methanogenic archaea and through the thermal degradation of organic molecules in sediments. A previous study indicated that the anaerobic biodegradation of organic compounds by hydrogen (H₂)-producing fermentative bacteria and H₂-utilizing methanogens contributes to the significant CH₄ reserves in deep aquifers associated with the accretionary prism in southwest Japan (20, 26, 29). However, regional variations in the CH₄ production process are poorly understood, in part because of insufficient data. In addition to CH₄, a large amount of nitrogen gas (N₂) is present in natural gas derived from deep aquifers. The origin of this N₂ remains elusive.

Therefore, the objectives of this study were to identify the origin of CH₄ reserved in deep aquifers in the Shimanto Belt by analyzing the stable isotopic signatures of groundwater and natural gas samples. We also examined the processes of and potential for microbial CH₄ and N₂ production using culture experiments and a DNA analysis. Collectively, the results from geochemical analyses and microbiological experiments were used to develop a model that explains regional variations in microbial activities and geochemical cycles in deep aquifers associated with the accretionary prism in southwest Japan.

Materials and Methods

Study sites and sample collection

Groundwater and natural gas samples were collected from 13 wells situated in Shizuoka Prefecture, Japan (Fig. 1). The wells were drilled down to deep aquifers associated with the accretionary prism

* Corresponding author. E-mail: kimura.hiroyuki@shizuoka.ac.jp;
Tel: +81-54-238-4784; Fax: +81-54-238-0491.

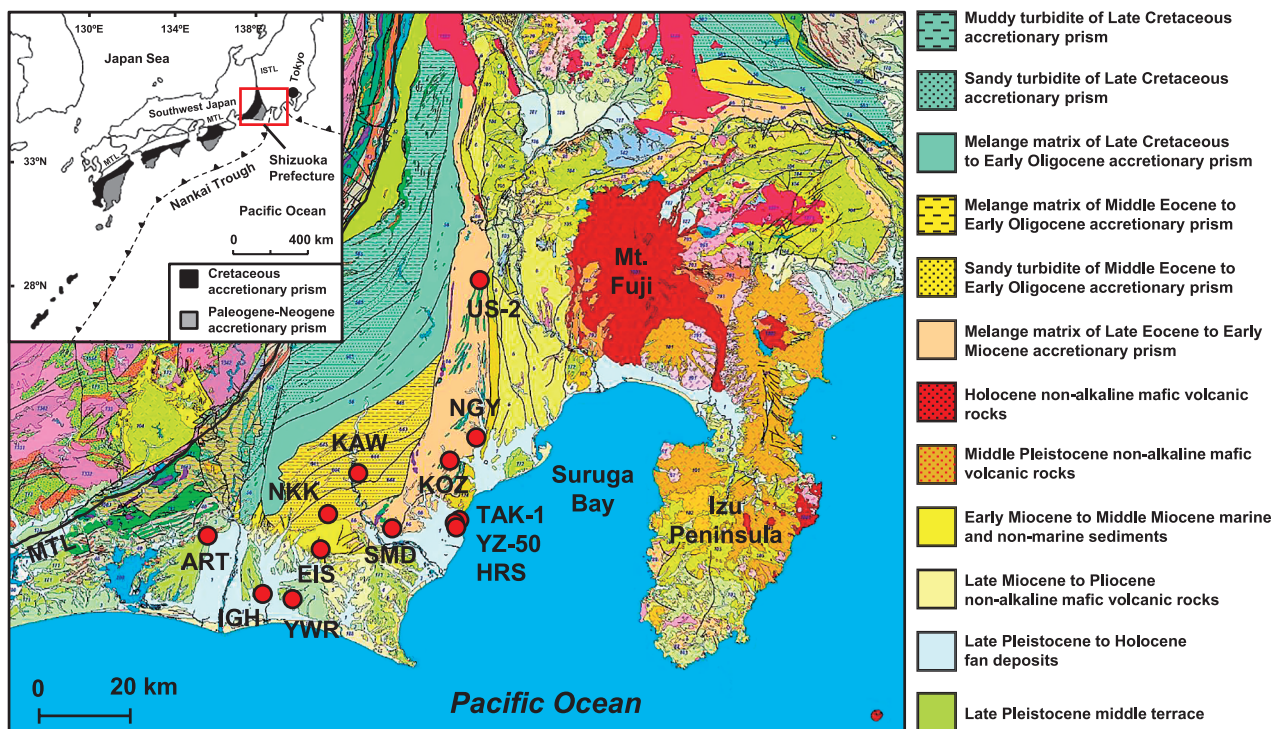


Fig. 1. Geological map of the study area. The location of the accretionary prism known as the Shimanto Belt in southwest Japan is according to Kano *et al.* (27). The geological map of Shizuoka Prefecture, Japan, is modified from the 1:200,000 seamless digital geological map of Japan (14). The circles indicate the locations of the wells used for sampling. MTL, Median Tectonic Line; ISTL, Itoigawa-Shizuoka Tectonic Line.

and constructed from tight steel-casing pipes including strainers (Table S1). Groundwater flows into these wells through parts of the strainers. Groundwater rises up to ground level by natural water pressure or is anaerobically drawn up to ground level by a water pump or gas lift system.

In order to prevent contamination by air and water from shallow environments, groundwater was pumped for 24 h before sampling. Groundwater samples were collected under anaerobic conditions into autoclaved serum bottles using a sterile silicone tube. The concentrations of dissolved natural gas were so high that gas exsolved at ground level. Natural gas samples were collected in an inverted funnel underwater and then directed into autoclaved serum bottles. Serum bottles were tightly sealed underwater with sterile butyl-rubber stoppers and aluminum crimps to prevent contamination by air.

Physical and chemical parameter measurements

The physical and chemical parameters of groundwater were measured at the outflow of the wells. Temperature was measured with a CT-460WR thermometer (Custom, Tokyo, Japan). Oxidation-reduction potential (ORP) and pH were measured with RM-20P and HM-20P portable meters (DKK-TOA, Tokyo, Japan), respectively. Electric conductivity (EC) was measured with a CM-21P portable meter (DKK-TOA).

The concentrations of anions (HCO_3^- , Cl^- , Br^- , I^- , F^- , NO_2^- , PO_4^{2-} , NO_3^- , SO_4^{2-} , acetate, and formate) and cations (Na^+ , K^+ , Mg^{2+} , Ca^{2+} , and NH_4^+) were measured using an ICS-1500 ion chromatography system (Dionex, Sunnyvale, CA, USA). Sulfide was analyzed using a methylene blue method (8). Total iron was measured using a modified version of the ferrozine method (54). Ferrous iron was quantified using a modified version of the 1,10-phenanthroline method (58). Spectrophotometric analyses for sulfide and irons were performed on site with a DR/2400 portable spectrophotometer (Hach, Loveland, CO, USA). Dissolved organic carbon (DOC) in groundwater filtered through pre-combusted GF/F glass microfiber filters (Whatman, Maidstone, UK, USA) was measured with a TOC-V total organic carbon analyzer (Shimadzu, Kyoto, Japan).

H_2 , N_2 , O_2 , N_2O , CO_2 , and CH_4 concentrations in natural gas were measured with a GC-2014 gas chromatograph (GC) (Shimadzu) equipped with a thermal conductivity detector (TCD) and packed column (ShinCarbon ST, 6.0 m \times 3.0 mm i.d.; Shinwa Chemical Industries, Kyoto, Japan). The GC conditions used were as follows: injector temperature, 170°C; column oven temperature, 150°C; detector temperature, 170°C. Argon (Ar) was used as a carrier gas at a constant flow mode of 50 mL min^{-1} . N_2 and Ar concentrations were measured with GC-2014 GC (Shimadzu) equipped with TCD and a packed column (Molecular Sieve 5A, 3.0 m \times 3.0 mm i.d.; Shinwa Chemical Industries). The GC conditions used were as follows: injector temperature, 50°C; column oven temperature, 40°C; detector temperature, 50°C. Helium was used as a carrier gas at a constant flow rate of 50 mL min^{-1} . CH_4 , C_2H_6 , and C_3H_8 concentrations were measured with GC-2014 GC (Shimadzu) equipped with a flame ionization detector and packed column (Sunpak-A, 2.0 m \times 3.0 mm i.d.; Shinwa Chemical Industries). The GC conditions used were as follows: injector temperature, 100°C; column oven temperature, 65°C; detector temperature, 100°C. N_2 was used as a carrier gas at a constant flow rate of 50 mL min^{-1} . Samples were analyzed in triplicate. Reference gases were analyzed at the start of each gas analysis. The confidence limits of the measurement were 0.01 vol.% for H_2 , N_2 , O_2 , N_2O , Ar, CO_2 , and CH_4 , and 0.001 vol.% for C_2H_6 and C_3H_8 .

Analysis of the stable carbon isotopic ratio

The stable carbon isotope ratio ($^{13}\text{C}/^{12}\text{C}$) of CH_4 in natural gas was measured with a Trace GC Ultra gas chromatograph (Thermo Fisher Scientific, Waltham, MA, USA) that was connected to a Delta V Advantage isotope ratio mass spectrometer (IRMS) with a GC IsoLink conversion unit and ConFlo IV interface (Thermo Fisher Scientific) (6).

The $^{13}\text{C}/^{12}\text{C}$ of total dissolved inorganic carbon (ΣCO_2) in groundwater, mainly bicarbonate, was analyzed as described previously (36). Groundwater samples for analyzing the $^{13}\text{C}/^{12}\text{C}$ of ΣCO_2 were fixed with 0.5 mL of saturated HgCl_2 solution and sealed with sterile butyl-rubber stoppers and aluminum crimps with no air bub-

bles. A 10-mL headspace was created inside each serum bottle with pure helium gas and acidified by adding CO₂-free H₃PO₄ solution. Sample bottles were left in the dark for 24 h to achieve equilibrium between dissolved CO₂ and headspace CO₂. CO₂ in this headspace was subsampled, and the ¹³C/¹²C ratio of CO₂ was measured by a Trace GC Ultra gas chromatograph (Thermo Fisher Scientific) that was connected to a Delta^{plus} XL IRMS (Thermo Fisher Scientific).

The stable isotope ratio was expressed in the conventional δ notation calculated from the equation

$$\delta = [R_{\text{sample}}/R_{\text{standard}} - 1] \times 1000 \text{ [‰]},$$

where *R* is the isotope ratio (¹³C/¹²C). The isotope ratio in this study is reported relative to the international standard, Vienna Pee Dee Belemnite (VPDB). The standard deviations of the δ¹³C of CH₄ and CO₂ were ±0.3‰ and ±1‰, respectively.

Total cell count and catalyzed reporter deposition fluorescence in situ hybridization (CARD-FISH)

The groundwater samples used for the total cell count were fixed in neutralized formalin (final concentration 1%). Ten milliliters of a groundwater sample was filtered using pre-blackened polycarbonate filters (pore size, 0.2 μm; diameter, 25 mm) (Millipore, Billerica, MA, USA). Microbial cells collected on the filter were stained with SYBR Green I (1:100 dilution) (Life Technologies, Carlsbad, CA, USA) (39). Microbial cells were observed under a model BX51 epifluorescence microscope equipped with a U-MNIB3 fluorescence filter (Olympus, Tokyo, Japan), and more than 50 microscopic fields (average 20–30 cells in each field) were counted for each sample. Cell counting was performed within 24 h of groundwater sampling.

Regarding CARD-FISH targeting archaeal and bacterial 16S rRNAs, groundwater samples were collected from eight wells (KAW, YZ-50, NKK, EIS, SMD, KOZ, US-2, and ART). CARD-FISH was conducted following the protocols reported by Mitsunobu *et al.* (35). Briefly, 50 mL of each groundwater sample was filtered with white polycarbonate membrane filters (pore size, 0.2 μm; diameter, 25 mm; Advantec, Tokyo, Japan). Cells on the filters were fixed in 3% paraformaldehyde and dehydrated in ethanol. The cells were then hybridized using the following horseradish peroxidase-labeled probes: *Bacteria*-specific EUB338 (2), *Archaea*-specific ARCH915 (52), and the control probe Non338 (60). In order to overcome the high autofluorescence of clay particles, cells were counterstained with SYBR Green I (Life Technologies). The Cy3-labeled tyramide signal was amplified using a TSA-Plus cyanine 3 system (Perkin Elmer, Waltham, MA, USA). Cell counting was performed with a model BX51 epifluorescence microscope (Olympus) equipped with a U-MNIG3 filter (Olympus) for hybridized cells and the U-MNIB3 filter (Olympus) for SYBR Green I-stained cells.

Next generation sequencer (NGS) analysis of 16S rRNA genes

In the NGS analysis, eight groundwater samples were collected from the same wells as those used in the CARD-FISH analysis. Ten liters of groundwater samples was aseptically filtered with Sterivex-GV filter units (pore size, 0.22 μm; Millipore) using a sterilized silicone tube and tubing pump (51). The bulk DNAs of microorganisms trapped by the filter units were extracted using a MORA-EXTRACT kit (Kyokuto Pharmaceutical, Tokyo, Japan). Bacterial and archaeal 16S rRNA gene fragments were simultaneously amplified from bulk DNA by PCR using the primer set, Pro341f and Pro806r based on the V3–V4 hypervariable region of the prokaryotic 16S rRNA gene (57). Library generation and sequencing using an Illumina Miseq sequencer were performed according to the method described by Takahashi *et al.* (57). Analyses of sequence reads were performed using the Ribosomal Database Project (RDP) Classifier Version 2.10 with a confidence threshold of 80% (61). The relative abundance of each phylogenetic group was assessed by the number of sequence reads affiliated with that group. In order to better estimate relative abundance, the number

of sequence reads affiliated with that group was adjusted based on the mean 16S rRNA gene copy numbers for that group provided by the rrnDB database (53).

In order to assess microbial diversity, sequence reads were grouped into operational taxonomic units (OTUs) sharing more than 97% sequence similarity, and alpha-diversity indices (Chao 1 and Shannon index) and coverage percentages were then calculated using the Quantitative Insights Into Microbial Ecology (QIIME) v 1.5.0 pipeline (7).

Measurements of potential microbial gas production

Autoclaved 70-mL serum bottles were tightly sealed with sterile butyl-rubber stoppers and aluminum crimps. Serum bottles were vacuum-pumped and then filled with pure N₂. After this process had been repeated four times, the serum bottles were vacuum-pumped again. Thirty milliliters of each groundwater sample was anaerobically injected into serum bottles with 35-mL syringes and needles.

In order to assess the potential for CH₄ production by methanogenic archaea, we prepared enrichments using groundwater amended with methanogenic substrates. Groundwater was supplemented with acetate (20 mM), methanol (20 mM), formate (20 mM), or H₂/CO₂ (80:20, v/v; 150 kPa). Except for H₂/CO₂-supplemented bottles, the headspaces of serum bottles were filled with pure N₂ at 150 kPa. Enrichments using groundwater amended with organic substrates were also prepared in order to evaluate the potential for microbial H₂ production via the anaerobic biodegradation of organic matter. Groundwater samples were amended with 3 mL of yeast extract, peptone, and glucose (YPG) medium (10 g of yeast extract, 10 g of peptone, and 2 g glucose L⁻¹ distilled water) and 20 mM of 2-bromoethanesulfonate (BES), an inhibitor of methanogens (29). The headspaces of the serum bottles were filled with pure N₂ at 150 kPa. We also measured the potential for CH₄ production by the syntrophic biodegradation of fermentative bacteria and methanogenic archaea. Groundwater samples were supplemented with 3 mL of YPG medium. In these enrichments, BES was not added. The headspaces of the serum bottles were filled with pure N₂ at 150 kPa.

The potential for N₂ production by denitrifying bacteria was also assessed. Groundwater samples were supplemented with 3 mL of YPG medium and nitrite (10 mM) or nitrate (10 mM). The headspaces of the serum bottles were filled with pure CH₄ at 150 kPa.

These enrichments were anaerobically incubated without shaking at each temperature of groundwater sample that was measured at the outflow of the well. Additionally, enrichments were incubated at temperatures that were 10°C higher than those of groundwater because the actual temperature in a deep aquifer is generally considered to be higher than that of groundwater measured at the outflow of the well (33, 43). H₂, N₂, N₂O, CH₄, and CO₂ concentrations in the headspace were measured with GC-2014 GC (Shimadzu) equipped with TCD and a ShinCarbon ST packed column (Shinwa Chemical Industries) as described above. Enrichments were performed in triplicate.

Microorganisms that grew in the enrichments in which biogas production was observed were identified according to the 16S rRNA gene clone library method described in a previous study (29). Briefly, cells in the enrichments were collected by centrifugation and bulk DNA was extracted. Archaeal and bacterial 16S rRNA gene fragments were amplified by PCR from bulk DNA using the *Archaea*-specific primer set, 109aF and 915aR (16, 52), and the *Bacteria*-specific primer set, 8bF and 1512uR (11), respectively. The sequences of the inserted PCR products selected from recombinant colonies were elucidated with an Applied Biosystems 3730xl DNA Analyzer (Life Technologies). The OTUs for each clone library were obtained using GENETYX-Mac ver. 17.0 (Genetyx, Tokyo, Japan). A 3% distance level between sequences was considered the cut-off for distinguishing distinct OTUs. We identified the nearest relative of each OTU using the BLAST program (1). Neighbor-joining phylogenetic trees based on Kimura's two-parameter model were constructed using the CLUSTAL X version 2.1 program and NJplot software (30, 31, 41, 44). The tree topology was evaluated by bootstrap resampling with 1,000 replicates.

Nucleotide sequence accession numbers

The 16S rRNA gene sequences obtained in this study have been deposited under GenBank/ENA/DDBJ accession numbers AB848725 to AB848733, AB985755 to AB985758, and DRA004556.

Results

Chemical and stable isotopic signatures of groundwater and natural gas

The temperature of groundwater was measured at the outflow of the deep well, and found to range between 24.2°C and 49.3°C (Table 1). pH was between 7.6 and 9.3. The ORP of groundwater indicated the anoxic conditions of deep aquifers associated with this accretionary prism. The EC, an indicator of salinity, varied between 110 mS m⁻¹ and 3,090 mS m⁻¹. Fe²⁺, Fe³⁺, PO₄²⁻, NO₂⁻, NO₃⁻, SO₄²⁻, S²⁻, acetate, and formate concentrations in groundwater were low or below the detection limits (Table S2).

In most of the natural gas samples obtained in this study, CH₄ was the predominant component, accounting for more than 96 vol.% (Table 1). Natural gas sampled from KAW, US-2, ART, and IGH included a large amount of N₂ (15–50 vol.%) as well as CH₄. Ar was detected in all natural gas samples (0.06–0.66 vol.%). The ratio of N₂ to Ar (N₂/Ar) was between 6 and 203. H₂, O₂, N₂O, CO₂, and C₃H₈ were below the detection limits.

The stable carbon isotope ratios of CH₄ in natural gas ($\delta^{13}\text{C}_{\text{CH}_4}$) and dissolved inorganic carbon in groundwater ($\delta^{13}\text{C}_{\Sigma\text{CO}_2}$), mainly bicarbonate, ranged between -69.4‰ and -33.5‰ and between -9.76‰ and 19.0‰, respectively (Table S3). Carbon isotope fractionation (α_c) between $\delta^{13}\text{C}_{\Sigma\text{CO}_2}$ and $\delta^{13}\text{C}_{\text{CH}_4}$ was between 1.025 and 1.076. We plotted stable isotopic values on a $\delta^{13}\text{C}_{\Sigma\text{CO}_2}$ versus $\delta^{13}\text{C}_{\text{CH}_4}$ diagram according to Smith and Pallasser (50). These values fell across regions of biogenic origin by microbial methanogenesis via CO₂ reduction, regions of thermogenic origin by abiotic CH₄ production, and the boundary area between the regions of biogenic origin and thermogenic origin (Fig. 2).

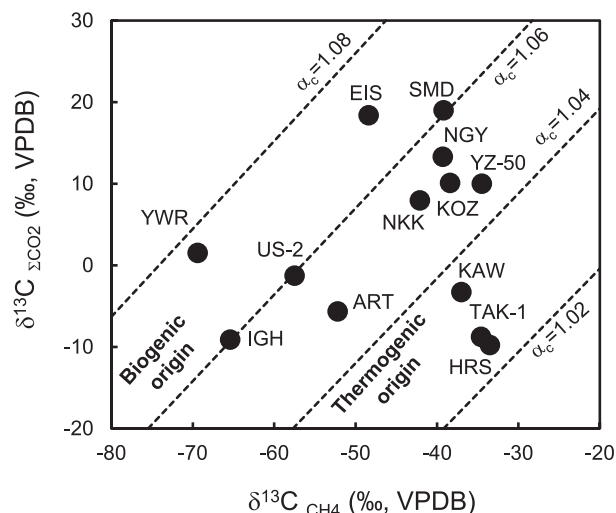


Fig. 2. Stable carbon isotope compositions of CH₄ in natural gas and dissolved inorganic carbon in groundwater. The broken lines of equal carbon isotopic fractionation, $\alpha_c = (\delta^{13}\text{C}_{\Sigma\text{CO}_2} + 10^3) / (\delta^{13}\text{C}_{\text{CH}_4} + 10^3)$, are drawn for $\alpha_c = 1.02, 1.04, 1.06,$ and 1.08 . The categorization of CH₄ origins is according to Smith and Pallasser (50). VPDB, Vienna Pee Dee Belemnite.

Abundance and diversity of microbial communities in groundwater

Microbial cell densities in groundwater samples ranged between 3.0×10^3 and 7.7×10^5 cells mL⁻¹ (Table 1). FISH-positive archaeal cells accounted for 5.5% to 68.0% of all microbial cells (Fig. S1 and Table S4). FISH-positive bacterial cells accounted for 7.1% to 45.2% of all microbial cells. The ratios of FISH-positive bacterial cells to archaeal cells (*Bacteria/Archaea*) ranged between 0.1 and 5.7.

Based on the NGS analysis, 7,787 to 33,274 reads and 128 to 787 OTUs were obtained (Table S5). The coverage percentage reached more than 98%. The Chao1 and Shannon indices ranged between 217 and 1,849 and between 1.18 and 6.25, respectively. The archaeal 16S rRNA genes showed the dominance of methanogens belonging to the order *Methanobacteriales*, an archaeal group that is known to use H₂ and CO₂ for growth and methanogenesis, in KAW, NKK, EIS, and SMD (Fig. 3A) (64). We also detected *Methanomassiliicoccales* and *Methanomicrobiales* as minor

Table 1. Physical and chemical parameters and microbial cell density of groundwater and components of natural gas.

Site code	Groundwater					Natural gas					
	Temp. (°C)	pH	ORP (mV)	EC (mS m ⁻¹)	Microbial cells (cells mL ⁻¹)	N ₂ (vol.%)	Ar (vol.%)	CH ₄ (vol.%)	C ₂ H ₆ (vol.%)	C ₃ H ₈ (vol.%)	N ₂ /Ar ratio
TAK-1	49.3	8.5	-175	3,090	3.0×10^3	2.86	0.18	97.0	0.028	n.d.	16
HRS	40.8	8.4	-183	2,590	7.7×10^5	1.18	0.19	98.6	0.016	n.d.	6
KAW	48.7	7.6	-196	2,450	4.5×10^3	15.8	0.25	83.8	0.061	n.d.	63
YZ-50	41.0	7.8	-114	2,050	2.7×10^4	1.98	0.10	97.9	0.018	n.d.	20
YWR	24.2	8.0	-226	1,747	1.7×10^4	1.19	0.06	98.7	0.009	n.d.	20
NKK	40.6	8.2	-178	1,619	5.6×10^4	2.37	0.07	97.5	0.152	n.d.	34
EIS	28.6	8.4	-312	586	4.0×10^4	2.46	0.08	97.4	0.063	n.d.	31
SMD	39.0	8.2	-270	559	1.4×10^4	0.79	0.06	96.9	2.248	n.d.	13
KOZ	30.0	8.3	-297	546	3.5×10^4	3.21	0.07	96.7	0.018	n.d.	46
NGY	26.7	9.3	-320	479	1.1×10^5	3.35	0.09	96.5	0.058	n.d.	37
US-2	32.8	8.9	-255	170	3.8×10^4	23.5	0.58	76.0	0.009	n.d.	41
ART	35.1	8.8	-257	147	2.5×10^4	50.2	0.25	49.5	0.015	n.d.	203
IGH	31.2	8.7	-265	110	1.2×10^4	36.4	0.66	63.0	0.004	n.d.	55

Abbreviations: ORP, oxidation-reduction potential; EC, electric conductivity; n.d. not detected.

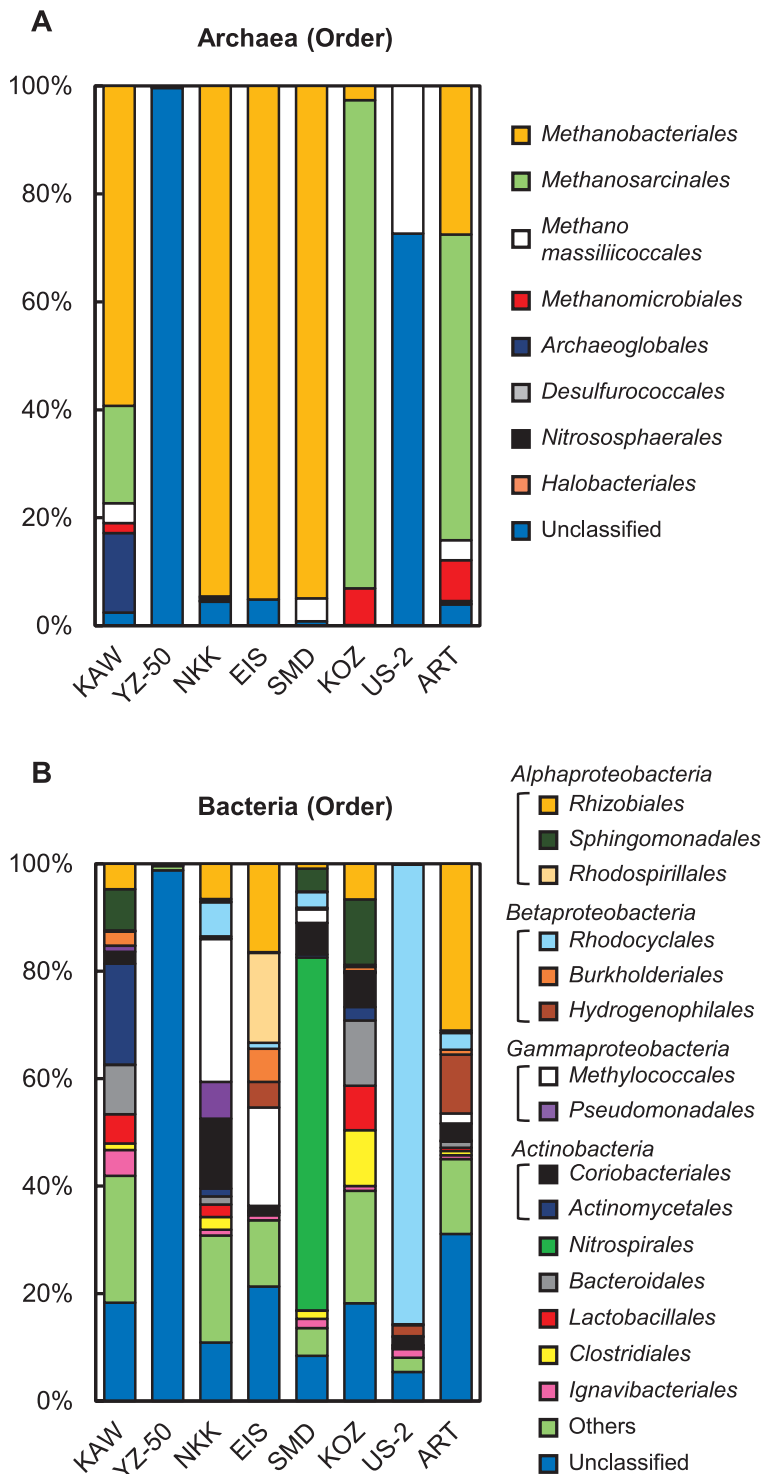


Fig. 3. Archaeal and bacterial assemblages in natural groundwater. (A) The relative abundance (%) of archaeal communities. (B) The relative abundance (%) of bacterial communities.

members of H₂-utilizing methanogenic archaea (10, 46). On the other hand, the dominance of the order *Methanosarcinales*, which is a methanogenic archaea that uses acetate as a methanogenic substrate, was also indicated in KOZ and ART (25). In contrast, a number of archaeal 16S rRNA genes obtained from YZ-50 and US-2 were unclassified archaea.

The NGS analysis of bacterial 16S rRNA genes demonstrated the dominance of the classes *Alphaproteobacteria*, *Betaproteobacteria*, and *Gammaproteobacteria* (Fig. 3B). The order *Rhizobiales* (*Alphaproteobacteria*), generally

known to comprise diazotrophs, was observed in most groundwater samples. We also confirmed the presence of the denitrifying bacterium *Rhodocyclales* (*Betaproteobacteria*) and aerobic methanotrophic bacterium *Methylococcales* (*Gammaproteobacteria*). The class *Actinobacteria* and orders *Nitrospirales*, *Bacteroidales*, *Lactobacillales*, *Clostridiales*, and *Ignavibacteriales*, which are bacterial groups containing anaerobic fermentative bacteria, were also identified (4, 18, 32, 38). A large number of bacterial 16S rRNA genes obtained from YZ-50 were unclassified bacteria.

Potential for microbial methanogenesis and fermentation

In order to assess the potential for CH₄ production by methanogens, we anaerobically incubated groundwater samples amended with methanogenic substrates: acetate, methanol, formate, or H₂/CO₂. CH₄ production was only observed in the enrichments amended with H₂/CO₂. CH₄ production was clearly observed in the enrichments using groundwater collected from NKK, SMD, and NGY, and incubations at temperatures that were 10°C higher than those measured at the outflow of the wells exhibited the strong potential for CH₄ production (Fig. S2 and S3).

We then performed enrichments using groundwater amended with YPG medium and BES in order to assess the potential for H₂ and CO₂ production mediated by fermentative bacteria. H₂ and CO₂ were detected in the gas phase of bottles within 48 h, except when enrichments using groundwater samples from TAK-1 and HRS were used (Fig. S4 and S5). Incubations at temperatures that were 10°C higher than those of groundwater measured at the outflow of the wells

exhibited a stronger potential for H₂ and CO₂ production.

In order to assess whether CH₄ is produced from organic substrates by the cooperative catabolism of H₂-producing fermentative bacteria and H₂-utilizing methanogens, we performed enrichments using groundwater supplemented with YPG medium. CH₄ production was not observed in the enrichments using groundwater obtained from TAK-1, HRS, and YZ-50 (Fig. 4 and S6). In contrast, in the enrichments using groundwater obtained from all other sites, H₂ and CO₂ were initially generated within 48 h and accumulated, and then H₂ decreased to below the detection limit. Following the disappearance of H₂, CH₄ production began to be observed. Incubations at temperatures that were 10°C higher than those of groundwater measured at ground level were suggested to exhibit a strong potential for CH₄ production. In order to identify microbes in the enrichments suggested to actively produce biogas, archaeal and bacterial 16S rRNA gene clone libraries were constructed. Enrichments using groundwater from YZ-50, KOZ, and ART were used in the 16S rRNA

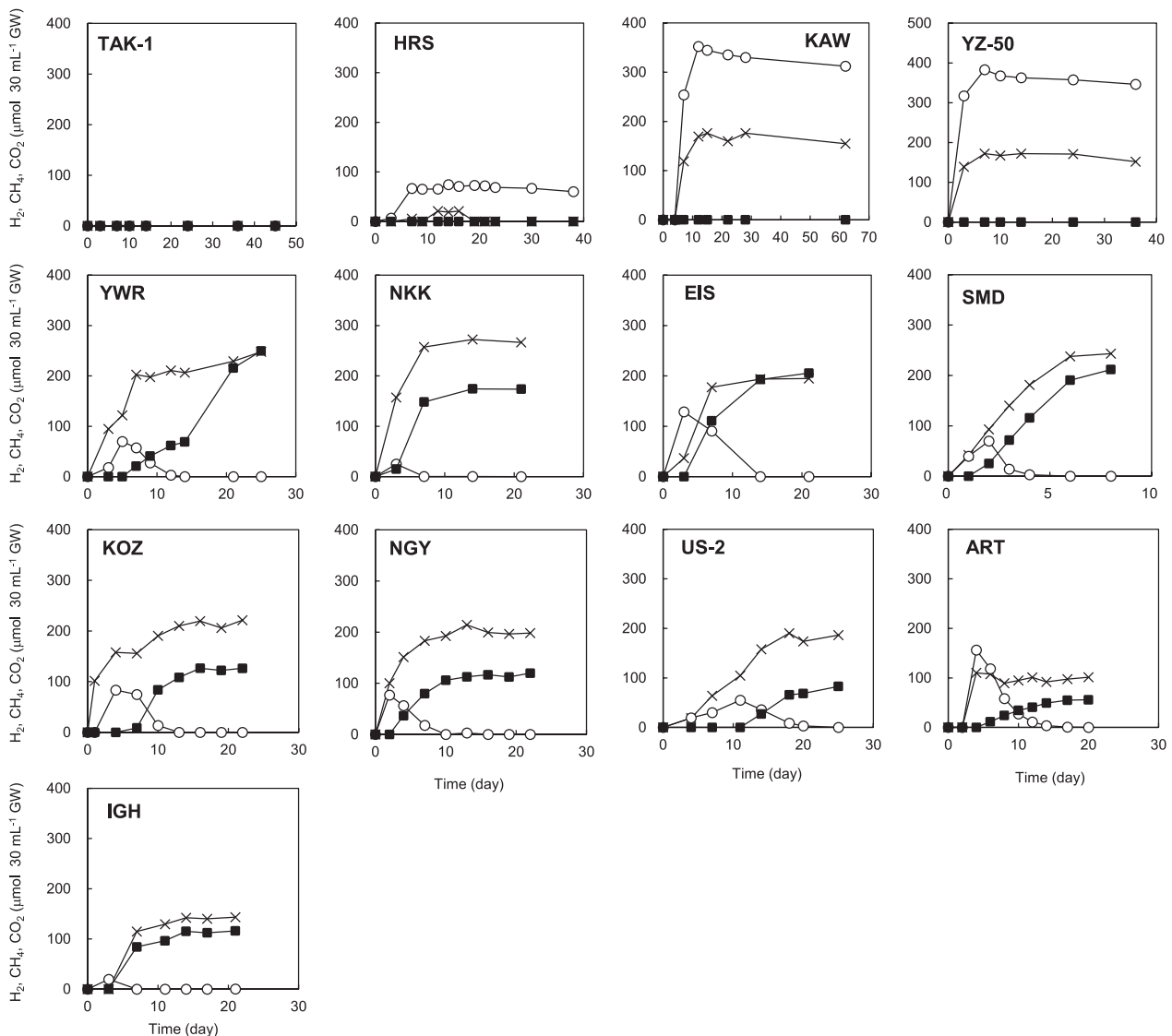


Fig. 4. Biogas production from groundwater samples amended with YPG medium incubated at temperatures that were 10°C higher than those of groundwater samples measured at the outflow of deep wells. Data points were obtained from the measurement of cumulative H₂ (○), CH₄ (■), and CO₂ (×) in the gas phase of the culture bottles.

gene analysis because the salinity of these groundwater samples had different signatures. The 16S rRNA gene analysis suggested that H₂-utilizing methanogenic archaea and H₂-producing fermentative bacteria were predominant in the enrichments, and that they belonged to the order *Methanobacteriales* and orders *Bacteroidales* and *Clostridiales*, respectively (4, 63, 64) (Fig. S7 and S8). The archaeal 16S rRNA gene was not amplified from the enrichment using groundwater obtained from YZ-50 by PCR after repeated attempts.

Potential for microbial denitrification

We tested the potential for N₂ production in deep aquifers associated with the accretionary prism. N₂ production was recently discovered in freshwater sediments and was shown to be mediated by anaerobic CH₄ oxidation coupled to denitrification (12, 42). In the present experiment, we used groundwater samples from US-2, ART, and IGH because large amounts of N₂ and CH₄ were detected in natural gas obtained from these sites. Consequently, N₂ was rapidly produced in the enrichments using groundwater supplemented with nitrate or nitrite and both CH₄ and YPG medium as electron donors (Fig. S9 and S10). A particularly strong potential for N₂ production was observed in the enrichments incubated at the temperatures of groundwater measured at ground level. In contrast, N₂ production was not observed in the enrichments amended with nitrate or nitrite and only CH₄ as an electron donor.

In order to elucidate the phylogenetic positions of the members with enhanced N₂ production induced by groundwater from the ART site, bacterial 16S rRNA genes derived from the enrichment were analyzed. The enrichment using groundwater from ART, which was supplemented with nitrate, CH₄, and YPG medium and was indicated to have the highest N₂ production rates, was used in the 16S rRNA gene analysis. The bacterial 16S rRNA genes revealed the dominance of the genus *Thauera* belonging to the order *Rhodocyclales* (Fig. S11). Species with validly published names in the genus *Thauera* have been isolated from various environments, and

these species are reported to be capable of nitrate reduction and denitrification using organic matter as electron donors under anaerobic conditions (34).

Discussion

TAK-1, HRS, and YZ-50 are located in a coastal region at an altitude of 2 m, close to Suruga Bay within the Philippine Sea subducting plate (Fig. 1 and Table S1). Natural gas from the three sites contained a high concentration of CH₄ (>97%). Our stable isotope analysis using the δ¹³C_{CH₄} versus δ¹³C_{ΣCO₂} diagram showed that CH₄ from the three sites is of thermogenic origin or is derived from both biogenic and thermogenic origins (Fig. 2). The enrichments using groundwater collected from the sites were indicated to have weak potential for CH₄ production by microbial communities (Fig. 4 and S6). We simply estimated the geothermal gradient at each sampling site based on the well depth and temperature of groundwater at the outflow of the wells (Table S1). HRS and YZ-50 were suggested to have markedly higher geothermal gradients than those of the other sites. These high geothermal gradients may have been due to faults or fractures associated with previous earthquakes that took place in Suruga Bay, close to the Tokai subduction zone (3). On the other hand, the geothermal gradient at the TAK-1 site was not particularly high. In the well at the TAK-1 site, groundwater is pumped up using a gas lift system, in which natural gas obtained from the deep aquifer is separated from groundwater, cooled for dehydration, and injected into the deep aquifer using a gas compressor (Table S1). Thus, groundwater from the well at TAK-1 is considered to be cooled by mixing with injected gas, and the actual geothermal gradient is higher than that calculated in this study (33°C km⁻¹). Our results based on the stable isotopic analysis, enrichments, and geothermal gradients suggest that CH₄ is generated by the breakdown of organic compounds through a thermogenic process in the deep aquifers of TAK-1, HRS, and YZ-50 located in the coastal area associated with the accretionary prism (Fig. 5).

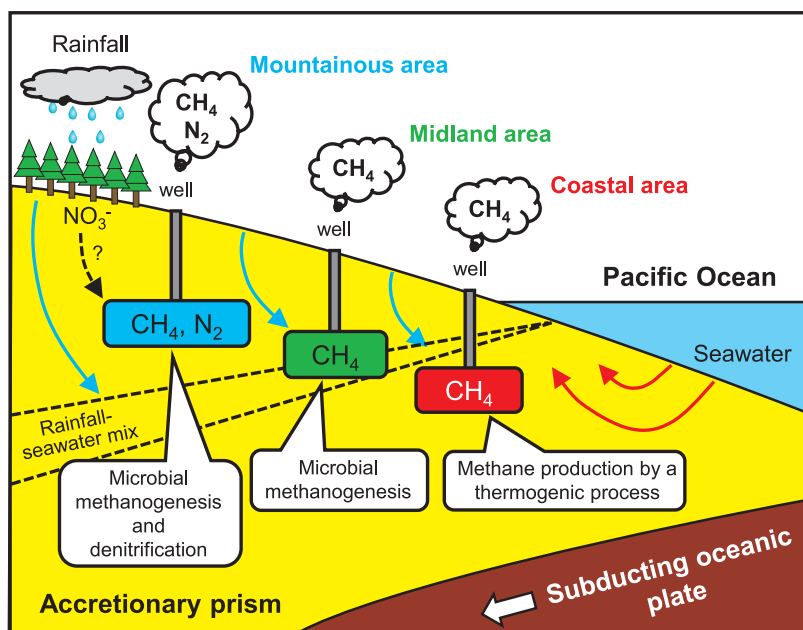


Fig. 5. Schematic of a groundwater flow model and CH₄ and N₂ production processes in deep aquifers of the coastal area, midland area, and mountainous area associated with the accretionary prism in southwest Japan.

On the other hand, the concentrations of the larger hydrocarbons (*e.g.*, C₂H₆) were low in natural gas obtained from the three sites (see Table 1), which is inconsistent with CH₄ production occurring through a thermogenic process (5). This result may have been due to non-methane hydrocarbons being stripped off during gas migration because larger hydrocarbons are more likely to be absorbed on sediment particles (47, 62).

Sites other than TAK-1, HRS, and YZ-50 are also located at an altitude of 24 m to 727 m in the midland or mountainous areas associated with the accretionary prism (Table S1). Natural gas collected from YWR, NKK, EIS, SMD, KOZ, and NGY contained high concentrations of CH₄ (>96 vol.%), whereas that from KAW, US-2, ART, and IGH contained CH₄ in the proportion of 49–83 vol.%. The stable carbon isotope ratios of CH₄ and ΣCO₂ from the ten sites ranged between –69.4‰ and –37.0‰ and between –9.10‰ and 19.0‰, respectively (Table S3). We noted the α_c value indicating offsets between δ¹³C_{ΣCO₂} and δ¹³C_{CH₄} because microbial CH₄ production in anaerobic subterranean environments is mainly mediated by H₂/CO₂-utilizing methanogenic archaea (29). α_c values varied from 1.04 to 1.08, except in the case of KAW, which suggests that CH₄ obtained from sites in the midland and mountainous area is biogenic in origin via H₂/CO₂-utilizing methanogenesis or is a mixture of biogenic and thermogenic origins (Fig. 2).

The CARD-FISH analysis targeting archaeal 16S rRNA suggested that archaeal cells are included at a proportion of 5.5% to 14.1% of all cells in groundwater samples. Additionally, the NGS analysis revealed the dominance of H₂-utilizing or acetate-utilizing methanogenic archaea in the archaeal communities. In order to measure the potential of CH₄ production by methanogens, we performed anaerobic cultivation using groundwater amended with methanogenic substrates. However, the strong potential for CH₄ production was only observed for the enrichments amended with H₂/CO₂ using groundwater collected from NKK, SMD, and NGY (Fig. S2 and S3). This may have been due to the growth inhibition of H₂-utilizing methanogens caused by the pH change in enrichments supplemented with H₂/CO₂ or by the use of a high concentration of methanogenic substrates (45).

The NGS analysis targeting bacterial 16S rRNA genes showed the presence of fermentative bacteria belonging to the orders *Nitrospirales*, *Bacteroidales*, *Lactobacillales*, *Clostridiales*, and *Ignavibacteriales* in groundwater. Previous studies reported that fermentative bacteria belonging to these bacterial groups are able to degrade organic matter to H₂ and CO₂ or acetate under anaerobic environments (4, 18, 32, 38). In addition, some species belonging to the classes *Alphaproteobacteria*, *Betaproteobacteria*, and *Gammaproteobacteria* have been shown to possess the ability to grow by fermentation under anaerobic environments (22, 24, 59). Our results suggest that these bacteria grow by fermentation and degrade organic matter to H₂ and CO₂ or acetate in deep aquifers, which is supported by enrichments using groundwater amended with YPG medium and BES having a strong potential for H₂ and CO₂ production (Fig. S4 and S5).

The biodegradation of organic matter under anaerobic conditions is achieved by the cooperative catabolism of

diverse bacteria and archaea. In particular, a syntrophic consortium between H₂-producing fermentative bacteria and H₂-utilizing methanogens is known to lead to the conversion of organic matter to CH₄ in anaerobic environments (40, 45, 49). Therefore, we tested the potential for CH₄ production by syntrophic biodegradation based on enrichments using groundwater amended with organic substrates. We observed rapid H₂ production/consumption and significant CH₄ production in these enrichments (Fig. 4 and S6). These dynamics of H₂ and CH₄ were clearly similar to those observed previously in syntrophic co-cultures of H₂-producing fermentative bacteria and H₂-utilizing methanogens (19, 29). Additionally, 16S rRNA gene analyses showed that H₂-producing fermentative bacteria and H₂-utilizing methanogenic archaea grew in these enrichments (Fig. S7 and S8). The results based on the stable isotopic analysis and microbiological assays strongly suggest that a syntrophic consortium of H₂-producing fermentative bacteria and H₂-utilizing methanogenic archaea contributes to CH₄ production in the deep aquifers in sites situated in midland and mountainous areas (Fig. 5). In addition, it currently remains unclear which chemical components of organic matter are actually used in this fermentation and CH₄ production. Future studies may identify these components.

The natural gas samples obtained from KAW, US-2, ART, and IGH contained large amounts of N₂ (15–50 vol.%). These sites are located at relatively high altitudes in the mountainous area associated with the accretionary prism. N₂ in natural gas may have been produced through microbial denitrification; nitrate is reduced to N₂ via the intermediate steps for nitrite, nitric oxide, and nitrous oxide (23). Nitrate was below the detection limit in groundwater obtained in this study, possibly due to a high level of nitrate consumption via the denitrification process. We herein measured N₂ and Ar concentrations in natural gas samples and calculated the N₂/Ar ratio. The amount of N₂ may be altered by biochemical reactions, whereas that of the noble gas Ar is expected to remain constant. If nitrate (or nitrite) is transformed into N₂ by microbial denitrification, the N₂/Ar ratio will be changed. The results of the gas analysis demonstrated that the N₂/Ar ratio ranged between 41 and 203 in natural gas collected from the four sites (Table 1). Air has an N₂/Ar ratio of 84, whereas air-saturated water has an N₂/Ar ratio of approximately 40 (9, 15). The N₂/Ar ratios of natural gas derived from the four sites were higher than that of air-saturated water.

N₂ production was not observed in the enrichments amended with nitrate or nitrite and only CH₄ as an electron donor using groundwater (Fig. S9 and S10). Therefore, denitrification coupled with anaerobic CH₄ oxidation may not occur in deep aquifers. On the other hand, the enrichments amended with nitrate or nitrite and organic matter and the 16S rRNA gene analysis suggest that denitrifying bacteria using organic matter as an electron donor exhibit a strong potential for N₂ production (see Fig. S9, S10, and S11). These results suggest that N₂ produced by microbial denitrification using organic matter is present in deep aquifers in sites located in the mountainous area (Fig. 5).

These denitrifying bacteria may compete with the CH₄-producing syntrophic consortium for organic matter in accretionary prism sediments. The competitiveness of denitrifying bacteria may be measured based on the amount

of nitrate present in the deep aquifer containing organic compounds, but only limited amounts of nitrate. Previous studies reported that excess amounts of nitrate are present in surface environments such as forest soil, and that it is lost via water movement (17, 48). Therefore, groundwater may deliver nitrate to deep aquifers associated with the accretionary prism. Although the KAW site was an exception, the salinity of groundwater obtained from US-2, ART, and IGH was significantly lower than that at the other sites ($P < 0.005$ by the Student's t -test). This result suggests that deep aquifers in the three sites were strongly affected by rainfall, and rainfall may supply them with nitrate, which is consistent with our detection of a significant amount of N₂ only from natural gas derived from the deep aquifer in the mountainous area.

Although natural gas obtained from KAW contained 15 vol.% of N₂, groundwater was indicated to have high salinity (2,450 mS m⁻¹). It has been proposed that a fault or fracture zone may be present at the KAW site (37). Therefore, the deep aquifer in the KAW site may be affected by rainfall and high-salinity groundwater that rises from the deep subterranean environment through fault or fracture zones. The clarification of groundwater flow in the subterranean environment associated with the accretionary prism will be an important topic for future study.

Conclusion

The chemical, stable isotopic, and microbiological data obtained in this study demonstrate regional variations in CH₄ and N₂ production processes. CH₄ is produced by a thermogenic process, particularly in the deep aquifer in the coastal area associated with the accretionary prism, and H₂-producing fermentative bacteria and H₂-utilizing methanogens contribute to the significant production of CH₄ in midland and mountainous areas. In addition, the production of N₂ in the deep aquifer in the mountainous area is mediated by denitrifying bacteria that use organic matter as an electron donor. Overall, these results lead us to the conclusion that dynamic groundwater flow and the ongoing biodegradation of organic matter in ancient sediments contribute to CH₄ and N₂ reserves in deep aquifers associated with the accretionary prism in southwest Japan.

Acknowledgements

We thank K. Someya, K. Yabuzaki, T. Ishida, T. Ohkubo, H. Yamamoto, M. Unno, T. Ito, M. Kobayashi, M. Sagisaka, K. Kaneko, M. Konagai, M. Mochizuki, and K. Ohsawa for their help with groundwater and natural gas sampling. This work was supported by the Japan Science and Technology Agency (JST) PRESTO and the Japan Society for the Promotion of Science (JSPS) KAKENHI Grant (no. 16H02968).

References

- Altschul, S.F., T.L. Madden, A.A. Schäffer, J. Zhang, Z. Zhang, W. Miller, and D.J. Lipman. 1997. Gapped BLAST and PSI-BLAST: a new generation of protein database search programs. *Nucleic Acids Res.* 25:3389–3402.
- Amann, R.L., L. Krumholz, and D.A. Stahl. 1990. Fluorescent-oligonucleotide probing of whole cells for determinative, phylogenetic, and environmental studies in microbiology. *J. Bacteriol.* 172:762–770.
- Aoi, S., B. Enescu, W. Suzuki, Y. Asano, K. Obara, T. Kunugi, and K. Shiomi. 2010. Stress transfer in the Tokai subduction zone from the 2009 Suruga Bay earthquake in Japan. *Nat. Geosci.* 3:496–500.
- Benno, Y., J. Watabe, and T. Mitsuoka. 1983. *Bacteroides pyogenes* sp. nov., *Bacteroides suis* sp. nov., and *Bacteroides helcogenes* sp. nov., new species from abscesses and feces of pigs. *Syst. Appl. Microbiol.* 4:396–407.
- Bernard, B.B., J.M. Brooks, and W.M. Sackett. 1978. Light hydrocarbons in recent Texas continental shelf and slope sediments. *J. Geophys. Res.* 83:4053–4061.
- Brand, W.A. 1996. High precision isotope ratio monitoring techniques in mass spectrometry. *J. Mass Spectrom.* 31:225–235.
- Caporaso, J.G., J. Kuczynski, J. Stombaugh, et al. 2010. QIIME allows analysis of high-throughput community sequencing data. *Nature Methods* 7:335–336.
- Cline, J.D. 1969. Spectrophotometric determination of hydrogen sulfide in natural waters. *Limnol. Oceanogr.* 14:454–458.
- de Moor, J.M., T.P. Fischer, Z.D. Sharp, D.R. Hilton, P.H. Barry, F. Mangasini, and C. Ramirez. 2013. Gas chemistry and nitrogen isotope compositions of cold mantle gases from Rungwe Volcanic Province, southern Tanzania. *Chem. Geol.* 339:30–42.
- Dridi, B., M.L. Fardeau, B. Ollivier, D. Raoult, and M. Drancourt. 2012. *Methanomassiliococcus luminyensis* gen. nov., sp. nov., a methanogenic archaeon isolated from human faeces. *Int. J. Syst. Evol. Microbiol.* 62:1902–1907.
- Eder, W., W. Ludwig, and R. Huber. 1999. Novel 16S rRNA gene sequences retrieved from highly saline brine sediments of Kebrut Deep, Red Sea. *Arch. Microbiol.* 172:213–218.
- Ettwig, K.F., M.K. Butler, D. Le Paslier, et al. 2010. Nitrite-driven anaerobic methane oxidation by oxygenic bacteria. *Nature* 464:543–548.
- Fagereng, Å. 2011. Fractal vein distributions within a fault-fracture mesh in an exhumed accretionary mélange, Chrystalls Beach Complex, New Zealand. *J. Struct. Geol.* 33:918–927.
- Geological Survey of Japan, AIST (ed.), 2014. Seamless digital geological map of Japan 1:200,000. Jan 14, 2014 version. Geological Survey of Japan. National Institute of Advanced Industrial Science and Technology, Ibaraki, Japan.
- Giggenbach, W.F. 1990. Water and gas chemistry of Lake Nyos and its bearing on the eruptive process. *J. Volcanol. Geoth. Res.* 42:337–362.
- Großkopf, R., P.H. Janssen, and W. Liesack. 1998. Diversity and structure of the methanogenic community in anoxic rice paddy soil microcosms as examined by cultivation and direct 16S rRNA gene sequence retrieval. *Appl. Environ. Microbiol.* 64:960–969.
- Gruber, N., and J.N. Galloway. 2008. An Earth-system perspective of the global nitrogen cycle. *Nature* 451:293–296.
- Haouari, O., M.L. Fardeau, J.L. Cayol, G. Fauque, C. Casiot, F. Elbaz-Poulichet, M. Hambi, and B. Ollivier. 2008. *Thermodesulfobacterium hydrogeniphilus* sp. nov., a new thermophilic sulphate-reducing bacterium isolated from a Tunisian hot spring. *Syst. Appl. Microbiol.* 31:38–42.
- Hattori, S. 2008. Syntrophic acetate-oxidizing microbes in methanogenic environments. *Microbes Environ.* 23:118–127.
- Hattori, S., H. Nashimoto, H. Kimura, K. Koba, K. Yamada, M. Shimizu, H. Watanabe, M. Yoh, and N. Yoshida. 2012. Hydrogen and carbon isotope fractionation by thermophilic hydrogenotrophic methanogens from a deep aquifer under coculture with fermenters. *Geochem. J.* 46:193–200.
- Hervé, F., M. Calderón, C.M. Fanning, R.J. Pankhurst, and E. Godoy. 2013. Provenance variations in the Late Paleozoic accretionary complex of central Chile as indicated by detrital zircons. *Gondwana Res.* 23:1122–1135.
- Hiraishi, A., Y. Hoshino, and T. Satoh. 1991. *Rhodiferax fermentans* gen. nov., sp. nov., a phototrophic purple nonsulfur bacterium previously referred to as the “*Rhodocyclus gelatinosus*-like” group. *Arch. Microbiol.* 155:330–336.
- Isobe, K., and N. Ohte. 2014. Ecological perspectives on microbes involved in N-cycling. *Microbes Environ.* 29:4–16.
- Kalyuzhnaya, M.G., S. Yang, O.N. Rozova, et al. 2013. Highly efficient methane biocatalysis revealed in a methanotrophic bacterium. *Nat. Commun.* 4:2785.

25. Kamagata, Y., H. Kawasaki, H. Oyaizu, K. Nakamura, E. Mikami, G. Endo, Y. Koga, and K. Yamasato. 1992. Characterization of three thermophilic strains of *Methanoxthrix* ("Methanosaeta") *thermophila* sp. nov. and rejection of *Methanoxthrix* ("Methanosaeta") *thermoacetophila*. *Int. J. Syst. Bacteriol.* 42:463–468.
26. Kaneko, M., Y. Takano, Y. Chikaraishi, *et al.* 2014. Quantitative analysis of coenzyme F430 in environmental samples: a new diagnostic tool for methanogenesis and anaerobic methane oxidation. *Anal. Chem.* 86:3633–3638.
27. Kano, K., M. Nakaji, and S. Takeuchi. 1991. Asymmetrical melange fabrics as possible indicators of the convergent direction of plates: a case study from the Shimanto Belt of the Akaishi Mountains, central Japan. *Tectonophysics* 185:375–388.
28. Karasawa, Y., and K. Kano. 1992. Formation and deformation process of the slate belt in the Setogawa Group (the Shimanto Belt) of the eastern Akaishi Mountains, easternmost Southwest Japan. *J. Geol. Society Japan* 98:761–777 (in Japanese with an English abstract).
29. Kimura, H., H. Nishimoto, M. Shimizu, S. Hattori, K. Yamada, K. Koba, N. Yoshida, and K. Kato. 2010. Microbial methane production in deep aquifer associated with the accretionary prism in Southwest Japan. *ISME J.* 4:531–541.
30. Kimura, M. 1980. A simple method for estimating evolutionary rates of base substitutions through comparative studies of nucleotide sequences. *J. Mol. Evol.* 16:111–120.
31. Larkin, M.A., G. Blackshields, N.P. Brown, *et al.* 2007. Clustal W and Clustal X version 2.0. *Bioinformatics* 23:2947–2948.
32. Liu, C., S.M. Finegold, Y. Song, and P.A. Lawson. 2008. Reclassification of *Clostridium coccoides*, *Ruminococcus hansenii*, *Ruminococcus hydrogenotrophicus*, *Ruminococcus luti*, *Ruminococcus productus* and *Ruminococcus schinkii* as *Blautia coccoides* gen. nov., comb. nov., *Blautia hansenii* comb. nov., *Blautia hydrogenotrophica* comb. nov., *Blautia luti* comb. nov., *Blautia producta* comb. nov., *Blautia schinkii* comb. nov. and description of *Blautia wexlerae* sp. nov., isolated from human faeces. *Int. J. Syst. Evol. Microbiol.* 58:1896–1902.
33. McLing, T.L., R.P. Smith, R.W. Smith, D.D. Blackwell, R.C. Roback, and A.J. Sondrup. 2016. Wellbore and groundwater temperature distribution eastern Snake River Plain, Idaho: Implications for groundwater flow and geothermal potential. *J. Volcanol. Geotherm. Res.* 320:144–155.
34. Mechichi, T., E. Stackebrandt, N. Gad'on, and G. Fuchs. 2002. Phylogenetic and metabolic diversity of bacteria degrading aromatic compounds under denitrifying conditions, and description of *Thauera phenylacetica* sp. nov., *Thauera aminoaromatica* sp. nov., and *Azoarcus buckelii* sp. nov. *Arch. Microbiol.* 178:26–35.
35. Mitsunobu, S., F. Shiraishi, H. Makita, B.N. Orcutt, S. Kikuchi, B.B. Jørgensen, and Y. Takahashi. 2012. Bacteriogenic Fe(III) (Oxyhydr) oxides characterized by synchrotron microprobe coupled with spatially resolved phylogenetic analysis. *Environ. Sci. Technol.* 46:3304–3311.
36. Miyajima, T., Y. Yamada, Y.T. Hanba, K. Yoshii, T. Koitabashi, and E. Wada. 1995. Determining the stable isotope ratio of total dissolved inorganic carbon in lake water by GC/C/IRMS. *Limnol. Oceanogr.* 40:994–1000.
37. Mogi, K. 1977. An interpretation of the recent tectonic activity in the Izu-Tokai district. *Bull. Earthq. Res. Inst.* 52:315–331 (in Japanese with an English abstract).
38. Nagai, F., Y. Watanabe, and M. Morotomi. 2010. *Slackia piriformis* sp. nov. and *Collinsella tanakaei* sp. nov., new members of the family *Coriobacteriaceae*, isolated from human faeces. *Int. J. Syst. Evol. Microbiol.* 60:2639–2646.
39. Noble, R.T., and J.A. Fuhrman. 1998. Use of SYBR Green I for rapid epifluorescence counts of marine viruses and bacteria. *Aquat. Microb. Ecol.* 14:113–118.
40. Noguchi, M., F. Kurisu, I. Kasuga, and H. Furumai. 2014. Time-resolved DNA stable isotope probing links *Desulfobacterales*- and *Coriobacteriaceae*-related bacteria to anaerobic degradation of benzene under methanogenic conditions. *Microbes Environ.* 29:191–199.
41. Perrière, G., and M. Gouy. 1996. WWW-Query: An on-line retrieval system for biological sequence banks. *Biochimie* 78:364–369.
42. Raghoebarsing, A.A., A. Pol, K.T. van de Pas-Schoonen, *et al.* 2006. A microbial consortium couples anaerobic methane oxidation to denitrification. *Nature* 440:918–921.
43. Saar, M.O. 2011. Review: Geothermal heat as a tracer of large-scale groundwater flow and as a means to determine permeability fields. *Hydrogeol. J.* 19:31–52.
44. Saitou, N., and M. Nei. 1987. The neighbor-joining method: a new method for reconstructing phylogenetic trees. *Mol. Biol. Evol.* 4:406–425.
45. Sakai, S., H. Imachi, Y. Sekiguchi, I.C. Tseng, A. Ohashi, H. Harada, and Y. Kamagata. 2009. Cultivation of methanogens under low-hydrogen conditions by using the coculture method. *Appl. Environ. Microbiol.* 75:4892–4886.
46. Sakai, S., M. Ehara, I.C. Tseng, T. Yamaguchi, S.L. Brauer, H. Cadillo-Quiroz, S.H. Zinder, and H. Imachi. 2012. *Methanolina mesophila* sp. nov., a hydrogenotrophic methanogen isolated from rice field soil, and proposal of the archaeal family *Methanoregulaceae* fam. nov. within the order *Methanomicrobiales*. *Int. J. Syst. Evol. Microbiol.* 62:1389–1395.
47. Sakata, S., T. Maekawa, S. Igari, and Y. Sano. 2012. Geochemistry and origin of natural gases dissolved in brines from gas fields in southwest Japan. *Geofluids* 12:327–335.
48. Shi, J., N. Ohte, N. Tokuchi, N. Imamura, M. Nagayama, T. Oda, and M. Suzuki. 2014. Nitrate isotopic composition reveals nitrogen deposition and transformation dynamics along the canopy–soil continuum of a suburban forest in Japan. *Rapid Commun. Mass Spectrom.* 28:2539–2549.
49. Shimoyama, T., S. Kato, S. Ishii, and K. Watanabe. 2009. Flagellum mediates symbiosis. *Science* 323:1574.
50. Smith, J.W., and R.J. Pallasser. 1996. Microbial origin of Australian coalbed methane. *AAPG Bull.* 80:891–897.
51. Somerville, C.C., I.T. Knight, W.L. Straube, and R.R. Colwell. 1989. Simple, rapid method for direct isolation of nucleic acids from aquatic environments. *Appl. Environ. Microbiol.* 55:548–554.
52. Stahl, D.A., and R. Amann. 1991. Development and application of nucleic acid probes in bacterial systematics, p. 205–248. *In* E. Stackebrandt, and M. Goodfellow (ed.), *Nucleic Acid Techniques in Bacterial Systematics*. John Wiley & Sons, New York.
53. Stoddard, S.F., B.J. Smith, R. Hein, B.P.K. Roller, and T.M. Schmidt. 2015. rrnDB: improved tools for interpreting rRNA gene abundance in bacteria and archaea and a new foundation for future development. *Nucleic Acids Res.* 43:D593–D598.
54. Stookey, L.L. 1970. Ferrozine—a new spectrophotometric reagent for iron. *Anal. Chem.* 42:779–781.
55. Taira, A., J. Katto, M. Tashiro, M. Okamura, and K. Kodama. 1988. The Shimanto Belt in Shikoku, Japan: evolution of Cretaceous to Miocene accretionary prism. *Mod. Geol.* 12:5–46.
56. Taira, A., T. Byrne, and J. Ashi. 1992. *Photographic Atlas of an Accretionary Prism: Geologic Structures of the Shimanto Belt*, Japan. University of Tokyo Press, Tokyo.
57. Takahashi, S., J. Tomita, K. Nishioka, T. Hisada, and M. Nishijima. 2014. Development of a prokaryotic universal primer for simultaneous analysis of bacteria and archaea using next-generation sequencing. *PLoS One* 9:e105592.
58. Tamura, H., K. Goto, T. Yotsuyanagi, and M. Nagayama. 1974. Spectrophotometric determination of iron(II) with 1,10-phenanthroline in the presence of large amounts of iron(III). *Talanta* 21:314–318.
59. Ueki, A., Y. Kodama, N. Kaku, T. Shiromura, A. Satoh, K. Watanabe, and K. Ueki. 2010. *Rhizomicrobium palustre* gen. nov., sp. nov., a facultatively anaerobic, fermentative stalked bacterium in the class *Alphaproteobacteria* isolated from rice plant roots. *J. Gen. Appl. Microbiol.* 56:193–203.
60. Wallner, G., R. Amann, and W. Beisker. 1993. Optimizing fluorescent in situ hybridization with rRNA-targeted oligonucleotide probes for flow cytometric identification of microorganisms. *Cytometry* 14:136–143.
61. Wang, Q., G.M. Garrity, J.M. Tiedje, and J.R. Cole. 2007. Naïve Bayesian classifier for rapid assignment of rRNA sequences into the new bacterial taxonomy. *Appl. Environ. Microbiol.* 73:5261–5267.
62. Waseda, A., and H. Iwano. 2008. Characterization of natural gases in Japan based on molecular and carbon isotopic compositions. *Geofluids* 8:286–292.
63. Zeikus, J.G., and R.S. Wolfe. 1972. *Methanobacterium thermoautotrophicus* sp. n., an anaerobic, autotrophic, extreme thermophile. *J. Bacteriol.* 109:707–713.
64. Zhu, J., X. Liu, and X. Dong. 2011. *Methanobacterium movens* sp. nov. and *Methanobacterium flexile* sp. nov., isolated from lake sediment. *Int. J. Syst. Evol. Microbiol.* 61:2974–2978.